Biorecognition through Layer-by-Layer Polyelectrolyte Assembly: In-Situ Hybridization on Living Cells

Anna L. Hillberg[†] and Maryam Tabrizian*[,†,‡,§]

Department of Biomedical Engineering, and Faculty of Dentistry, Duff Medical Science Building, 3775 University Street, McGill University, Montreal, H3A 2B4, Canada

Received March 20, 2006; Revised Manuscript Received July 14, 2006

Encapsulated cells were formed from the assembly of cationic and anionic alternating layers using a number of polyelectrolyte-based systems. Chitosan, alginate, hyaluronic acid, and oligonucleotides were used as polyelectrolytes to encapsulate individual *E. coli* cells, which were used as a model. Zeta potential measurements taken for both chitosan/alginate and chitosan/hyaluronic acid systems indicate successful layer-by-layer (LbL) deposition and gave full reversal of the surface change eight times. Layer adsorption was further observed by fluorescence microscopy, and, through a newly developed protocol for sample preparation, transmission electron microscopy micrographs clearly showed the presence of LbL assembly on the outer layer of the cell membrane, in the nanometer range. A second generation of *E. coli* cells could be grown from encapsulated first generation cells, demonstrating that the cellular activity was not affected by the presence of polyelectrolyte multilayers. Hybridization between attached oligonucleotide sequences and the complementary sequence was demonstrated by both fluorescence spectroscopy and microscopy. Fluorescence energy transfer data recorded after hybrid formation showed that at a molar ratio of 10:20 (donor:acceptor), *Q* and *I* were 92.3% and 52.5%, respectively, which suggests that fluorescein fluorescence was quenched by 92.3% and that the fluorescence of rhodamine was enhanced by 52.5%. Oligonucleotide incorporation was stabilized by deposition of four alternating layers, hence offering not only the potential use of the encapsulated cell as a bio-recognition system but also its application in a number of fields such as oligonucleotide delivery, gene therapy, and the use of DNA as an immunocompatible coating.

I. Introduction

Layer-by-layer (LbL) assembly is a technique that has been used extensively in the preparation of multilayer films.[1−7] With the LbL deposition procedure, several hundred consecutively alternating polyelectrolyte layers have successfully been assembled on flat surfaces, and research has proven these films to be easy to prepare on a multitude of substrates. Resultant layers have been uniform, continuous, hard wearing, easily tailored, and in certain cases resistant to protein adsorption.

Polyelectrolyte layers are known to camouflage substrate defects, yielding a system with many ionic bonds and good adhesion properties.[1,8−15] Layer thickness, the mechanism of multilayer growth (linear or exponential), and the surface conformation of these polyelectrolyte multilayers are independent of the underlying substrate size and topology. These characteristics, along with surface roughness and the homo- or heterogeneity of such films, are also influenced by additional factors, including the ionic concentration and chemical nature of the polyions, the pH of all solutions, and the amount of time spent in polyelectrolyte solutions.[1−3,15−22] The LbL process can utilize water-soluble molecules, and consequently multicomponent films can be produced that can be used in the biological and medical fields, and therefore this process can be viewed as an alternative to Langmuir−Blodgett (LB) and self-assembly modification (SAM) techniques, which are frequently used for the preparation of sensing surfaces.[3,23,24]

The LbL technique was first used to produce a bio-recognition system and/or sensing element by Decher et al., who investigated template guided deposition of streptavidin in alternation with co-poly(L-lysine)(ϵ-biotinyl-L-lysine) on a flat surface, which was patterned by photoablation.[15,25] Immobilization of streptavidin enabled the controlled attachment of biotinylated molecules and thus allowed for the immobilization of a multitude of functional molecules on the modified surface. A similar bio-recognition system was also used for the electrochemical detection of glucose.[26] Lvov et al. used this technique to produce ultrathin (100−500 Å) films, laying down alternating layers of DNA as a polyanion and poly (allylamine) as a polycation. They aimed to utilize these films as sensing devices for various specific reagents for DNA, with possible applications in biological and ecological fields.[3] They also demonstrated controlled adsorption of water-soluble proteins within multicomponent films.[4]

The large amount of success achieved in producing "functional systems" by deposition of polyelectrolytes on flat surfaces incited researchers to extend LbL assembly onto three-dimensional and colloidal surfaces, with defined interfacial features and functionality.[27−32] Radtchenko et al. demonstrated that decomposition of the polyelectrolyte template creates a selectively permeable hollow capsule.[33] The micro- and macro-melamine formaldehyde particles, which were used as a template, were dissolved by a reduction in the pH, leaving capsules with the dimensions of the template.[34,35] Caruso et al. took this technique one step further and loaded hollow polyelectrolyte capsules with enzymes.[36,37] Such systems, demonstrating selective permeability, could find use in the field of drug delivery as an alternative to liposomes, due to their resistance to chemical and physical influences.[30,38−40] Nanoparticles have also been encapsulated using the LbL approach, with a view to facilitate capsule manipulation and tracking.[41−43] Hua et al. used the electrostatic LbL approach to coat platelets

* Corresponding author. Tel.: (514) 398-8129. Fax: (514) 398-7461. E-mail: maryam.tabrizian@mcgill.ca.
† McGill University.
‡ Centre for Biorecognition and Biosensors.
§ McGill Institute for Advanced Materials.

10.1021/bm060266j CCC: $33.50
Published on Web 09/20/2006

with silica nanoparticles, fluorescent nanospheres, or bovine immunoglobulin G (IgG).[44] The nanoassembly of Bovine IgG on platelet surfaces was verified with anti-bovine IgG-FITC labeling, and the localized targeting of anti-IgG shelled platelets was demonstrated.[44] A number of researchers have used this method of microcapsule formation and evaluated polyelectrolyte-coated red blood cells as a means of sustained drug release.[44,45] It may also be interesting to coat living cells to protect them from immune attack and keep them alive, or guide them to specific sites within the body.[46,47] An investigation with living yeast cells demonstrated that, after encapsulation, cells preserved their metabolic activity and were still able to divide, but in doing so caused destruction of the polyelectrolyte coat.[47] Mak et al. also reported on the cell surface engineering of yeast using layers of polyelectrolytes and layers of lactate oxidase. The outer enzyme layer provided an additional biological function for the yeast cells and aided in the conversion of lactate into pyruvate.[48]

In this paper, we have explored the use of the LbL assembly technique to coat living cells and to prove the concept that such a system is stable and could be used as a bio-recognition element. First, we used three biocompatible polysaccharides,[49] chitosan (polycation), either in combination with sodium alginate or hyaluronic acid (HA) (polyanions). These polyion pairs were used to encapsulate individual living *E. coli* cells. Chitosan [(1→4)-2-amino-2-deoxy-β-D-glucan] is a natural polymer with a pK_a of between 6.3 and 7.0. Its polyelectrolyte properties have enabled its use in the LbL surface modification of two- and three-dimensional surfaces.[4,15,17,20,21,28−31,36−38,50−55] Alginate is a linear, anionic, unbranched polymer, which has great potential for use in drug delivery systems and in the field of tissue engineering. It contains β-(1→4)-linked D-mannuronic acid (M) and (1→4)-linked L-guluronic acid (G) residues.[56−59] HA is a naturally occurring, highly biocompatible, anionic glycosaminoglycan, which consists of alternating *N*-acetyl-β-D-glucosamine and β-D-glucuronic acid residues, linked (1→3) and (1→4), respectively. It has been used as a polyion when the LbL technique has been employed to bioengineer anti-fouling surfaces and as a promising way to improve the haemocompatibility of blood-contacting surfaces.[48,60,61]

As mentioned, layer-by-layer encapsulated cells will eventually find application in a multitude of scientific fields, while encapsulated bacteria open up new avenues of research. For example, chitosan has excellent chelation properties, and bacteria are frequently employed within the field of environmental protection for the removal of heavy metals from solution. Bacteria encapsulated within layers of chitosan and other polyelectrolytes may have future applications within this field as a means of enhancing heavy metal immobilization.[62] Also, bacteria are known to enter mammalian cells via microbial pathogenesis. In this process, microbial cells adhere to the host cell wall and are eventually taken up by mammalian cells via either phagocytosis or bacterial-induced endocytosis (invasion). It has been shown that after internalization many microbial pathogens end up in mammalian cell cytoplasm.[63,64] If we can manipulate microbial pathogenesis as a means of targeting and delivery, we may be able to use it in future applications in the fields of drug, gene, and oligonucleotide delivery.

In parallel, we investigated the deposition of deoxyribonucleic acid (DNA) in alternation with chitosan as a biorecognition element for DNA hybridization. DNA is polyanionic because of the negative charge carried by the sugar−phosphate backbone. Its potential as a polyelectrolyte has been demonstrated repeatedly.[65,66] For example, the interaction between DNA and oppositely charged surfactants was investigated by Lindman et al., who demonstrated DNA compaction and adsorption on the surfaces of positively charged vesicles. Addition of an anionic surfactant caused the release of DNA back into solution from the compact globular complex. They also investigated the interaction of DNA with chitosan and concluded that generally any chitosan that is effective in promoting DNA compaction is also effective in transfection.[66]

For all approaches investigated within this paper, the surface charge of coated cells was monitored during the LbL process after the deposition of each successive layer, using zeta potential analysis. Layer adsorption was further investigated by fluorescence microscopy. Cell and capsule morphology were analyzed by transmission electron microscopy (TEM). Cell viability was assessed by monitoring the growth of encapsulated cells over a 24 h period. Fluorescence techniques, spectrophotometry, microscopy, and fluorescence resonance energy transfer (FRET), were also used to observe polyelectrolyte and oligonucleotide (ODN) attachment and hybridization.

II. Experimental Section

II.1. Reagents and Materials. The bacteria *Escherichia coli* (*E. coli*), strain HB101, was supplied by American type Culture collection (ATCC). Luria-Bertani (LB) agar and 2xYT culture medium were obtained from Fisher. Sodium hydrogen phosphate (Na_2HPO_4), potassium hydrogen phosphate (KH_2PO_4), sodium chloride (NaCl), magnesium sulfate ($MgSO_4$), thiamine hydrochloride ($C_{12}H_{17}ClN_4OS\cdot HCl$), and glucose were supplied by Sigma-Aldrich. Casamino acids were purchased from Fisher. Ampicillin (Fisher) was suspended in ultrapure water and further purified using a 0.22 μm syringe filter. Phosphate buffered saline tablets were supplied by Sigma-Aldrich. Triton (x100) and trizma base were used in the preparation of 10xTE buffer (Sigma-Aldrich). 2% saline sodium citrate (SSC) buffer was prepared from 20× stock solution purchased from Fisher. Sodium dodecyl sulfate (SDS) (Fisher) was used to make up 0.2% SDS phosphate buffer. The chitosan ($M_w \approx 10-500\,000$ kDa) and alginate were purchased from Medipol, Switzerland, and hyaluronic acid was purchased from CarboMer, Inc. For confocal fluorescence microscopy and spectroscopy measurements, fluorescein isothiocyanate (FITC)-labeled chitosan and hyaluronic acid were used (CarboMer, Inc.). ODNs were purchased from Integrated DNA Technologies. The purity of the DNA was verified by absorbance spectroscopy (OD_{260}) and used without further purification.

II.2. Medium Preparation. M9 minimal medium was prepared from 6 g of Na_2HPO_4, 3 g of KH_2PO_4, 0.5 g of NaCl in 1 L of ultrapure water, autoclaved and supplemented with 1 M $MgSO_4$, 20% (w/v) glucose, 1% casamino acids, and 2 mg/mL thiamine, and the pH was adjusted to 7.4.

II.3. Polyelectrolyte Solutions. 1 and 2 mg/mL chitosan (M_w 10−500 000 kDa) solutions were made up in 0.1% acetic acid, 0.1 M NaCl, and the pH was adjusted to 6.5. 1 mg/mL alginate and HA solutions containing 0.1 M NaCl were prepared in ultrapure water, and the pH was adjusted to 5.8 and 6.0, respectively. All polyelectrolytes formed solutions.

II.4. Cell Growth. A single colony of *E. coli* HB101 was picked from an agar plate grown at 37 °C. This was then grown up in 5 mL of 2xYT media containing 100 μg/mL of ampicillin, in a shaking incubator at 37 °C overnight. This culture was then used to inoculate a 1-L flask containing 500 mL of M9 minimal media and ampicillin (50 μg/mL). The culture was grown at 37 °C under constant shaking until stationary phase was reached at an OD_{600} of 0.6−1.0. The optical density of the culture was measured against sterile M9 medium. The cell density was measured via the plate spreading technique using 4% w/v LB agar plates. Serial dilutions of the cell culture were prepared in the range 1/500−1/125, and 100 μL of each dilution was evenly spread over the surface of the agar. The plates were then inverted and

incubated at 37 °C to allow the cells to grow in single colonies. The number of colonies formed was counted for each dilution, and the average cell number was calculated per milliliter of solution.

II.5. Cell Surface Modification. The cells were harvested by centrifugation at 4000 rpm at 4 °C for 25 min and washed four times in 0.1 M phosphate buffer saline (PBS), pH 6.5. Centrifugation was used to separate the cells from the supernatant. After each spin, the supernatant was discarded and the cell pellet was resuspended in PBS. LbL assembly of polyelectrolytes onto negatively charged *E. coli* cells was carried out as follows: an 8:1 (v/v) ratio of cells in 0.1 M PBS, pH 6.5 was mixed with 1 mg/mL of polycationic chitosan solution, prepared in 0.1% acetic acid, 0.1 M NaCl, pH 6.5. The cells were suspended immediately by vortexing for 5 s and agitation for 20 min at 37 °C. The cells were then allowed to stand for 5 min at room temperature. To separate chitosan free in solution from polyelectrolyte-encapsulated cells, the suspension was centrifuged lightly (4000 rpm for 5 min). The upper layer was discarded, and the bottom layer was resuspended in PBS. This washing step was repeated until no free chitosan remained in solution (four times). Initial experiments monitored the removal of free chitosan using fluorescence spectroscopy. The resulting chitosan-encapsulated cells were then further coated with alginate, HA, or DNA. Negatively charged alginate solution was prepared in 0.1 M PBS, 0.1 M NaCl, pH 5.8. Adsorption was carried out as described for the deposition of chitosan. For the adsorption of HA (polyanion), the positively charged chitosan-coated cells were resuspended as a 4:1 (v/v) ratio of coated cells to HA (0.1 M PBS, 0.1 M NaCl, pH 6.0). Adsorption of polyanionic ODNs was carried out using a 1:1 (v/v) ratio of chitosan-encapsulated cells to DNA. LbL polyelectrolyte deposition was carried out by repeated alternative deposition of these oppositely charged polyions.

II.6. Fluorescence Resonance Energy Transfer (FRET) Investigation. *Oligonucleotides.* Two 20-mer ODNs were used in these studies: a donor ODN (5′-TCCCGCCTGTGACATGCATT-3′) labeled at the 5′ end with fluorescein (FAM), and the complementary sequence (target) (5′-AGGGCGGACACTGTACGTAA-3′) labeled at the 3′ end with rhodamine (TAMRA), both supplied by Integrated DNA Technologies, Inc., Coralville, USA. Appropriate concentrations of the ODNs were prepared in PBS (10 mM phosphate buffer and 100 mM NaCl, pH 7).

FRET Experiment. The control sample was 10 μM of donor ODN attached to chitosan-modified *E. coli* cell surfaces, in the absence of the acceptor compound. The acceptor compound (TAMRA) was added to samples containing the donor compound adsorbed on the surface of modified cells. Donor:acceptor molar ratios of 10:20 and 20:20, in a 1:1 volume ratio, were examined and compared to the control. The samples were lightly agitated (120 rpm) overnight at 37 °C. Emission spectra were recorded using a GEMINI XS model microplate reader (Molecular Devices, Sunnyvale, CA) equipped with a temperature control chamber at 37 °C, between 500 and 600 nm with excitation at 470 nm. λ_{exc} of fluorescein was 470 and 540 nm for rhodamine. The λ_{emi} values for fluorescein and rhodamine were 522 and 580 nm, respectively. In all experiments, the background fluorescence of the phosphate buffer was negligible. Fluorescein fluorescence quenching (Q) was calculated as follows: $Q = (1 - (F_{(donor+acceptor)}/F_{(donor)})) \times 100$, where F = fluorescence level at 520 nm. The rhodamine fluorescence increase value (I) was computed as $I = (F'_{(donor+acceptor)}/F'_{(donor)} + F'_{(acceptor)})) \times 100$, where F' = fluorescence level at 580 nm. All of the results are expressed as percentages.

II.7. Hybridization Assay. First, the complementary ODN sequence (5′-TCCCGCCTGTGACATGCATT-3′) was bound to the outer surface of the chitosan-encapsulated *E. coli* cells. ODN target sequence (5′-AATGCATGTCACAGGCGGGA-3′) was diluted in TE buffer to a range of concentrations (0.5−0.05 μmol/L) and was allowed to hybridize with its complementary sequence (attached to cell surface) in a 1:1 (v/v) ratio. Hybridization took place in a shaking incubator overnight at room temperature in 2% SSC buffer. After hybridization, samples were washed four times in 0.2% SDS phosphate buffer and resuspended in TE buffer. Target DNA was labeled at the 5′ end of the ODN with a fluorescent tag (cytochrome 5), and hybridization was analyzed using fluorescence spectroscopy and microscopy. All assay solutions were measured against a blank. The blank was composed of cells that were encapsulated with an inner layer of chitosan, and an outer layer of ODN, and suspended in the corresponding buffer. Different cell to complementary sequence ratios (volume/volume (mL)) were investigated (1:1, 1:2, 1:4, and 1:6).

II.8. Zeta Potential Measurements. The electrophoretic mobility of the samples was measured using a ZetaPlus zeta potential analyzer (Brookhaven Instruments Corp.) ($n = 10$ for each measurement).

II.9. Fluorescence Spectroscopy. Fluorescence spectra were recorded using an FL_x800 microplate fluorescence reader (BIO-TEK instruments Inc.). FITC λ_{exc} was set at 490 nm, and λ_{emi} was set at 520 nm. Cytochrome 5 fluorescence was measured using a GEMINI XS model microplate reader (Molecular Devices, Sunnyvale, CA). λ_{exc} was set at 643 nm, and λ_{emi} was set at 667 nm.

II.10. Fluorescence Microscopy. *E. coli* cells were washed three times in 0.1 M PBS buffer, 0.1 M NaCl, pH 6.5, then resuspended in 2.5% glutaraldehyde solution (Fluka) and left to stand overnight at −4 °C (cell fixation). After fixation, the cells were washed three times in PBS buffer. Nuclear [4′,6′-diamidino-2-phenylinodole dihydrochloride (DAPI)] and polyelectrolyte capsule [fluorescein isthiocyanate (FITC)] fluorescence was detected by exciting cells with a UV light at ∼365 nm (DAPI) and 490 nm (FITC). A LSM ZEISS 510 confocal microscope was used to image polyelectrolyte encapsulated cells and unmodified cells using a 100× oil immersion objective lens. DAPI (10 μM; Invitrogen) was used for nuclear visualization. Slides were mounted using Permafluor mountant (Thermo Electron Corp.).

II.11. Transmission Electron Microscopy (TEM). TEM images were captured with a Tecnai 12 120 kV microscope. All samples were fixed prior to sample preparation and analysis (see section II.10). Following fixation, the cells were dehydrated using a graded series of acetone (25%, 30%, 50%, 75%, 80%, 90%, and 100%). Embedding involved resuspending the dehydrated cells in various ratios of Epon to acetone (1:1 overnight, 2:1 for 4 h, 3:1 overnight, and pure Epon for 4 h, before embedding in fresh and pure Epon).

II.12. Cell Viability. The viability of *E. coli* cells after polyelectrolyte encapsulation was studied by monitoring cell growth. Encapsulated cells were grown up in 5 mL of 2xYT media containing 100 μg/mL of ampicillin, in a shaking incubator at 37 °C overnight. This culture was then used to inoculate a 1-L flask containing 500 mL of M9 minimal media and ampicillin (50 μg/mL). The culture was grown at 37 °C under constant shaking until stationary phase was reached at an OD_{600} of 0.6−1.0. The optical density of the culture was measured against sterile M9 medium. Images were captured using fluorescence microscopy.

III. Results and Discussion

In this study, we established a technique for the assembly of polyelectrolyte capsules of predetermined composition around single cells, via LbL adsorption. The protocol involved the immersion of the cells in solutions of a number of anionic and cationic compounds: proteins and linear polyelectrolytes. Volume/volume (v/v) ratios of the two components (polyelectrolyte and cells) were varied depending on the electrolyte coating being deposited and the concentration of the solution applied.

III.1. Zeta Potential Measurements. The sign of the ζ-potential indicated an overall negative charge for bacterial cell surfaces by virtue of ionized phosphoryl and carboxylate groups on macromolecules situated on the outer cell wall, which are exposed to the extracellular environment. This negative surface charge provided a suitable template for the deposition of oppositely charged components and the successive LbL adsorption of alternating polyelectrolytes. After the adsorption

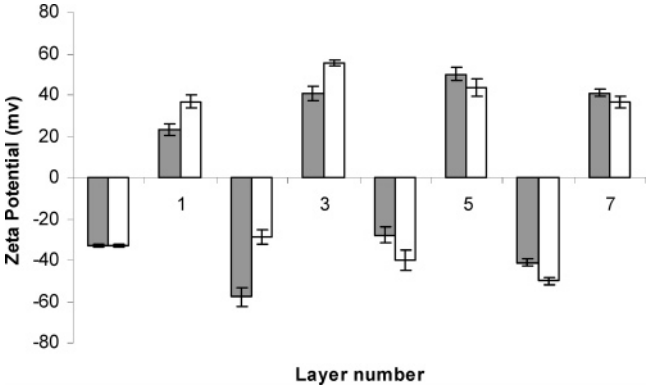

Figure 1. Charge alternation with successive deposition of polyelectrolytes chitosan (polycation) and □ = alginate or ■ = hyaluronic acid (polyanions), where layer 0 refers to the charge of the cell membrane. Measurements were taken using a zeta potential analyzer.

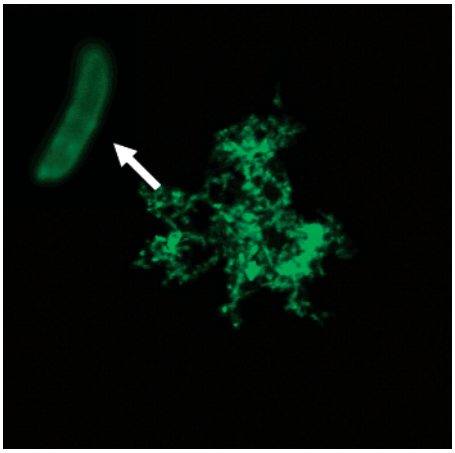

Figure 2. Confocal microscope images of *E. coli* cells encapsulated with chitosan−FITC/alginate LbL deposition (100× magnification, oil immersion lens). The figure in the left corner shows a single *E. coli* cell coated with polyelectrolytes.

of oppositely charged chitosan, the ζ-potential reverted to a positive charge of magnitude similar to that observed for the negatively charged bacterial cell surface. Successive adsorption of the anionic polymer, either sodium alginate or HA, resulted in a negative surface of comparable magnitude. The chitosan−alginate (or chitosan−HA) LbL encapsulation approach was shown to give full reversal of the surface charge eight times, which corresponds to seven layers of polymer (Figure 1). Similar results have been shown in numerous articles involving the deposition of a variety of polyelectrolyte systems on various templates. Caruso looked into the formation of nanoparticle/polymer multilayers on polystyrene lattices, in which the polymer layers were composed of poly(diallyldimethylammonium chloride) (PDADMAC) and poly(styrenesulfonate) (PSS).[67] He also investigated the formation of nanoparticle/polymer layers formed from SiO_2 nanoparticles and PDADMAC.[67] Other work analyzed using this method includes: the formation of DNA/spermidine layers on melamine formaldehyde (MF) colloidal particles,[68] encapsulation of water-soluble organic crystals of pyrene and fluorescein diacetate, using poly(allylamine hydrochloride) (PAH) and poly(sodium 4-styrenesulfonate) (PSS),[69] core−shell particle formation consisting of a polystyrene (PS) latex colloidal core and Fe(II) metallo-supramolecular polyelectrolyte (Fe(II)-MEPE)/PSS multilayer shells,[70] and the LbL deposition of PAH and PSS onto charged polystyrene latex particles.[71]

III.2. Spectroscopy and Microscopy Studies. Evidence for the LbL encapsulation of *E. coli* was further demonstrated by fluorescence spectroscopy and confocal fluorescence microscopy. Fluorescein isthiocyanate (FITC)−chitosan was used in the preparation of chitosan−alginate structures (Figure 2), while FITC−HA (figure not shown) was substituted in the preparation of chitosa−HA-coated cells. An increase in fluorescence originating from the surface of the polymer-coated cell was observed after the addition of each successive FITC-labeled layer, indicating successful polymer deposition. The fluorescence images also indicated that the cell size, shape, and structural morphology were retained after cell encapsulation and that the cells were engulfed within a layer of polymer. Evidence for complete cell encapsulation and the maintenance of cell integrity was previously demonstrated by Diaspro et al., who used this approach to coat yeast cells within layers of PSS and FITC-labeled PAH.[47]

In agreement with fluorescence microscopy observations, our TEM images showed that encapsulation of the individual cells did not alter their structure (Figure 3A). The ability of the LbL technique to effectively coat cells without altering the morphology was also shown in an original research by Neu et al. when analyzing the morphology of red blood cells coated with PAH and PSS. However, the method used by Neu et al. involved LbL adsorption of polyions onto chemically stabilized cells (fixed), rather than living cells.[35] In addition, Mak et al. used scanning electron microscopy to investigate the morphology of encapsulated living *Arxula adeninivorans* (yeast). They concluded that encapsulation did not result in the breakdown of the template structure and that no difference in surface morphology was observed between the encapsulated and untreated cells.[48] Our TEM images reveal that the encapsulating shell is in the nanometer range but the thickness of shell varies over the entire surface of the cell, thus providing a very heterogeneous surface, which is globular in structure (Figure 3B). Figure 3A shows a complete cell coated with polymer, which is shown in black, and the cell membrane is shown in white. The inset within Figure 3A is a longitudinal section through a bacterial cell, while the main image is a transverse section. From the comparison of TEM micrographs of control cells (Figure 3C) and encapsulated cells, it was possible to evaluate the coating thickness in the range 24−60 nm for $[\text{chitosan/alginate}]_2$ and 25−40 nm for $[\text{chitosan/hyaluronic acid}]_2$ systems (figure not shown). Recently, Feng et al. investigated polyelectrolyte self-assembly of HA/chitosan films on oppositely charged surfaces and used AFM to investigate how self-assembly order affects film topology and roughness.[72] Their results suggested that mica surfaces coated with chitosan/HA polyions produced heterogeneous films with a height variation between 60 and 100 nm, and a surface roughness of 16 nm. They also noted the formation of polyelectrolyte clusters at the film surface. Our values and those obtained by Feng et al. differ greatly from measurements observed by Sukhorukov et al. for the encapsulation of cross-linked MF colloidal particles, who found that 9 consecutive layers of PSS and PAH gave a polyelectrolyte film thickness of approximately 20 nm.[71] However, TEM and SEM images obtained by Sukhorukov and his group did show that the outer surface of the polyelectrolyte film was rough, and had no distinct layer structure, which parallels results obtained in this work.[71] Globular features observed at the film/capsule surface (Figure 3B) may well be polyion pair complexes, which form as a result of the attractive interactions between polyelectrolytes. These complexes form after the deposition of the second polyion (HA or alginate).

Early work on LbL deposition involving highly charged polyelectrolytes PSS/PAH suggested that layer thickness in-

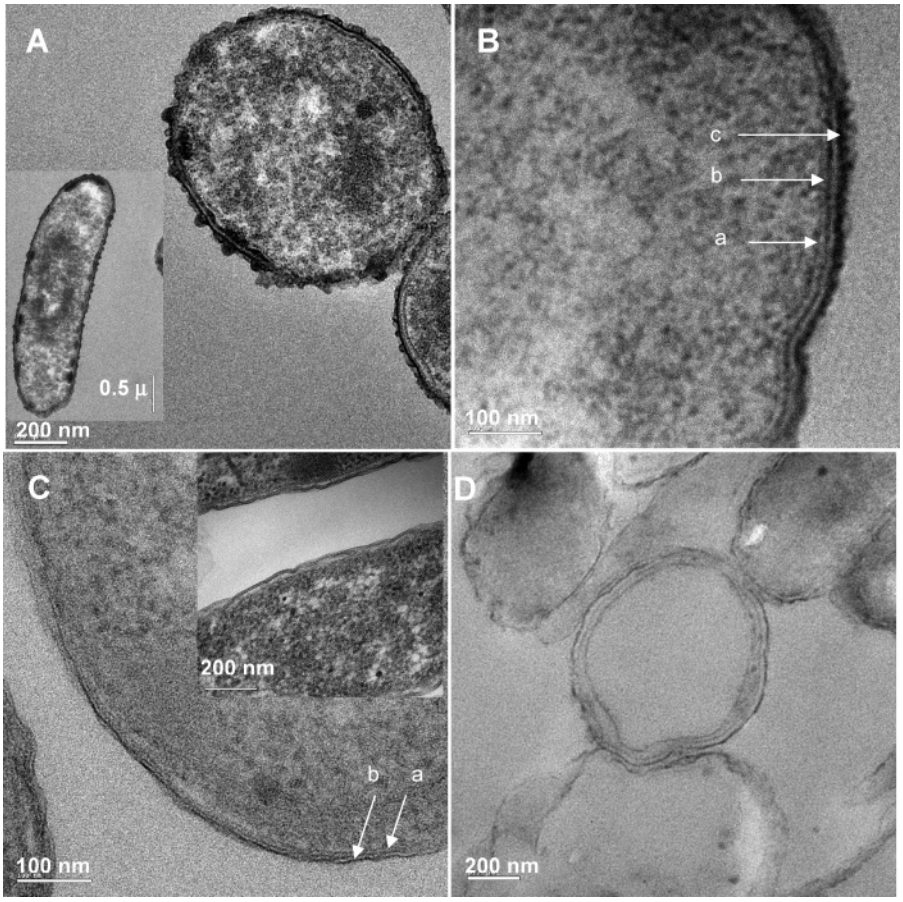

Figure 3. TEM micrographs of *Esherichia coli* coated with [chitosan/alginate]$_2$ shells. (A) Transverse section of a single cell showing the polyelectrolyte layers are stained black and can clearly be identified when compared to the inner and outer cell membranes, which appear white. A typical single cell (longitudinal section) having a mean length of 3 μm and diameter of approximately 1 μm with the intact morphology illustrated in the inset. (B) Magnification of a section of image A showing individual layers: a = inner cell membrane, b = outer cell membrane, and c = polyelectrolyte. The polyelectrolyte layer thickness varies from cell to cell and within a single cell coating, within the range 24−60 nm. (C) A cross-section of uncoated cell used as control: a = inner cell membrane, b = outer cell membrane. (D) Hollows of polyelectrolytes [chitosan/hyaluronic acid]$_4$ after cell lysis.

creased linearly with the amount of polymer deposited;[73] however, more recent experimental evidence has shown that different polyion combinations and increased ionic concentrations can lead to exponential growth. This was demonstrated by Lavalle et al., who investigated the structure and growth of polyelectrolyte multilayer films exhibiting linear growth (PSS/PAH) and exponential growth ((poly(L-glutamic acid)/poly(L-lysine)) (PGA/PLL)), with the aim of finding a correlation between surface roughness and the mechanism of growth. They concluded that the mechanism of growth influences the thickness of the polymer film, and nonspecific and/or weak polymer-to-polymer interactions lead to an increase in film thickness.[21] The thickness of the capsules developed here may suggest that they are candidates for exponential growth. The zeta potential measurements also show a high magnitude of ζ-potential, which is usually associated with the formation of a stable complex.[44] However, if this system is growing exponentially, then this could indicate the formation of an ever-changing complex, with polymer chains moving in and out of the system.[21]

Furthermore, TEM analysis also revealed that the LbL coating is stable and could be maintained after cell lysis (Figure 3D), suggesting the potential use of hollow capsules as biomacromolecule presenting systems, because the inner layer of the polyelectrolyte capsule could be used as template for membrane components.

III.3. Cell Viability and Growth. The viability of *E. coli* was studied before and after encapsulation by staining with 4′,6′-diamidino-2-phenylinodole dihydrochloride (DAPI). DAPI is a low molecular weight fluorescent dye, which penetrates the capsule and the cell wall, and binds to nuclear and mitochondrial DNA.[47] This procedure can be regarded as a means to verify cell structure preservation. Observation of encapsulated stained cells by fluorescence microscopy indicated that the cells were still viable after polyelectrolyte encapsulation (Figure 4). We also studied the cells' ability to divide and grow while encapsulated within numerous layers of polyelectrolyte. The cells were incubated at 37 °C in 2xYT growth medium overnight. The spectrophotometric measurements confirmed an increase in turbidity, which is consistent with cell growth. The presence of polyelectrolyte within the growth medium did not complicate the measurement due to the fact that chitosan absorbs at a wavelength of ~280 nm, while cell growth was monitored at 600 nm. To eliminate any possible complications that may arise from the presence of displaced chitosan, all measurements were blanked against initial conditions (e.g., first generation encapsulated *E. coli* cells). The growth curve shows a lag phase of approximately 6−8 h for all conditions (Figure 4). Cells that were not encapsulated reached steady-state between 8 and 10 h, while cells that had previously been encapsulated within polyelectrolyte demonstrated increased growth, and after 12 h steady-state had still not been reached. We suggest that the presence of chitosan within the growth medium stimulates bacterial cell growth as it is a great source of carbon and nitrogen. Interestingly, *E. coli* cells encapsulated within FITC−

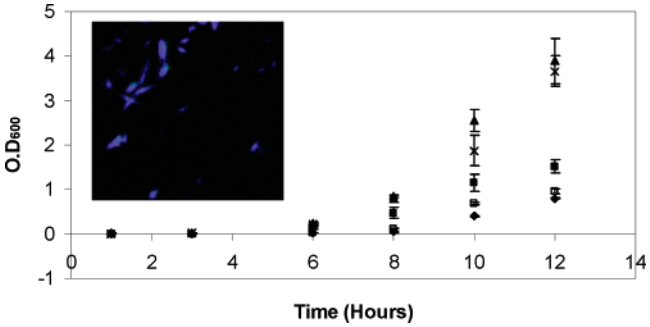

Figure 4. Growth of second generation *E. coli* cells. ▲ = first generation cells resuspended in PBS and encapsulated in 1 mg/mL chitosan (8:1 ratio of cell:chitosan); × = *E. coli* cells resuspended in PBS and encapsulated with 2 mg/mL chitosan; ◆ = first generation cells in 2xYT media; ■ = first generation cells resuspended in PBS and coated with FITC-labeled chitosan; □ = *E. coli* cells resuspended in PBS and grown up in 2xYT media. Inset shows the fluorescent detection of nuclear and mitochondrial DNA (DAPI staining), following polyelectrolyte capsule formation.

chitosan were also grown up in cell culture conditions, and second generation *E. coli* cells were visualized by fluorescence microscopy (figure not shown). We found that the intensity of the fluorescence was reduced in the second generation of encapsulated *E. coli* cells, which could be attributed to the increase in the cell population without an increase in the concentration of fluorescently labeled polymer. This hypothesis is strengthened by the fact that Diaspro et al. also found that the second generation of yeast were a heterogeneous mix of fluorescently labeled cells, cells without fluorescence, and very few fluorescent mother cells with mainly nonfluorescent buds.[47] Altogether, our data emphasized the fact that chitosan, alginate, and HA were noncytotoxic and could be used as polyelectrolytes in the LbL coating of living cells without causing damage to the cell morphology, viability, and metabolic activities. However, cells that are actively able to divide and multiply within a polyelectrolyte capsule will ultimately bring about other complications, given that cell division obviously disturbs polyelectrolyte multilayers. Following cell division, charged cell surfaces should still be able to interact with oppositely charged polyelectrolytes, which are found in the surrounding solution; nevertheless, this will eventually lead to a decrease in the thickness of the capsule wall. Permeability of polyelectrolyte capsules may be tailored by varying the electrolytic ionic strength and/or pH of polyion solutions.[74] This might allow us to control the flux of molecules entering and exciting polyelectrolyte capsules. If we can find a way to control the specific cell permeability, we may be able to control cell division while hopefully maintaining cell viability.

III.4. Biorecognition through DNA Hybridization. Hybridization studies were carried out with the aim of demonstrating the electrolytic potential of DNA as an immunogenic and natural polyelectrolyte that can be used in LbL assembly, and the effectiveness of such a system as a bio-recognition element. First, a 20-mer ODN modified by the attachment of cytochrome 5 (at the 5′ end) was adsorbed onto the surface of the chitosan-coated cells. Multilayer assembly of alternating layers of chitosan and DNA enabled the formation of a four-layer complex surrounding *E. coli* cells (Figure 5A). Fluorescence imaging shown in Figure 5B proved adsorption of the ODN to the surface of individual *E. coli* cells. Attempts to increase the number of layers resulted in a decrease in the ζ-potential and deemed the complex unstable. This might be caused by the large dilution to the system resulting from the multitude of consecutive centrifugation and washing steps that are used as a means of

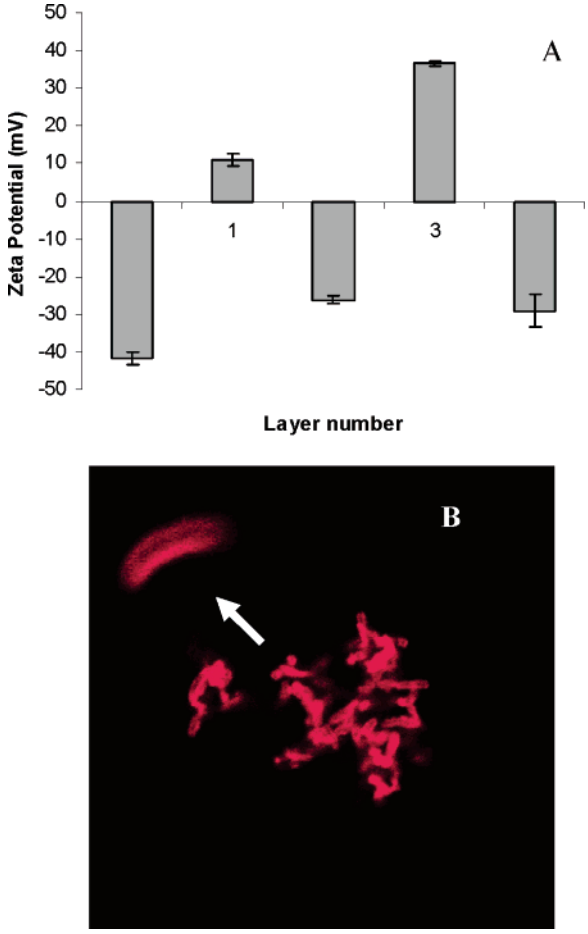

Figure 5. (A) Zeta potential measurement showing the charge alternation with successive deposition of chitosan (polycation) and DNA (polyanion), where layer 0 refers to the charge of the cell membrane. (B) Confocal microscope images of *E. coli* cells encapsulated with a layer of positively charged chitosan and a second layer of negatively charged cytochrome 5-labeled oligonucleotide (100× magnification, oil immersion lens). A single coated *E. coli* cell is illustrated in the inset.

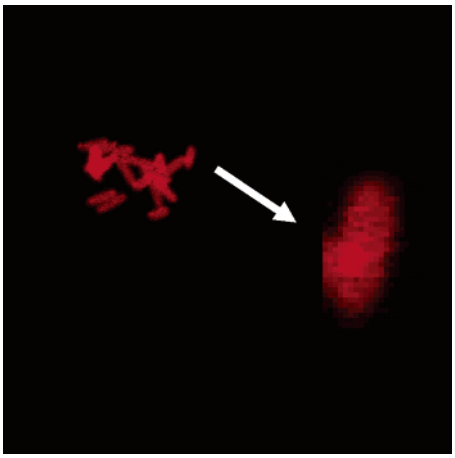

Figure 6. Hybridization demonstrated by specific binding of cytochrome 5 5′-labeled oligonucleotide.

removing unattached polyelectrolyte. Second, the DNA hybridization assay demonstrated specific binding between the unlabeled sequence of DNA (attached to the cell surface) and the complementary sequence (labeled with cytochrome 5), which was found in solution. Images shown in Figure 6), which were taken after hybridization and washing/centrifugation steps, demonstrated that the complementary sequence is still bound

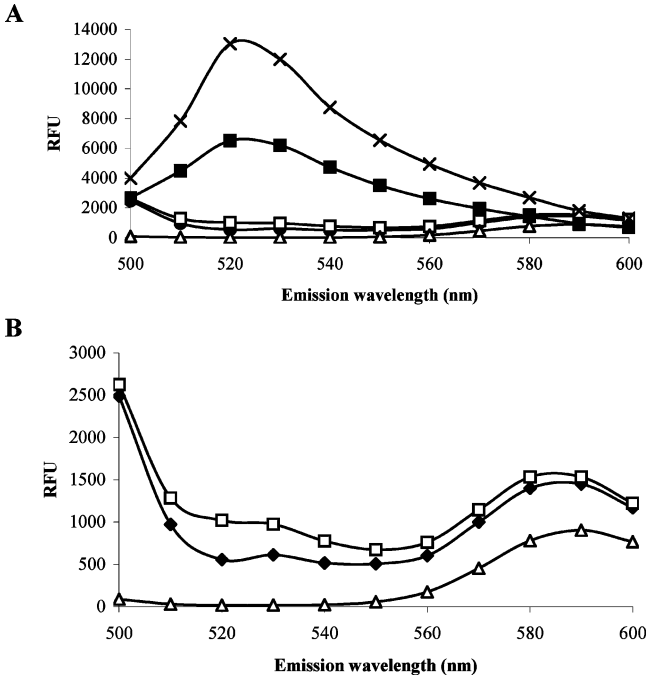

Figure 7. Emission spectra of the donor and acceptor compounds alone and in combination, at different molar ratios. (A) Donor compound (FAM) attached to modified cell surface at 20 μM (−×−); donor compound attached to cell surface at 10 μM (−■−); acceptor compound labeled with TAMRA, 20 μM (−△−); 20:20 molar ratio of donor and acceptor (−□−); 10:20 molar ratio of donor and acceptor (−◆−). (B) Fluorescence spectra of TAMRA alone (−△−) and FRET results: 20:20 molar ratio of donor and acceptor (−□−); 10:20 molar ratio of donor and acceptor (−◆−).

to the modified cell surface and hence hybridized with the target sequence.

III.5. Fluorescence Resonance Energy Transfer (FRET) Studies. We also investigated DNA hybridization through the use of FRET.[75−77] FRET involves the transfer of energy from a donor on one probe to an acceptor on the other. If the two are in close proximity, excitation of the donor results in energy transfer to the acceptor. Sixou et al. used FRET to study hybrid formation and dissociation after microinjection of ODNs into living cells. A 28-mer sense ODN was labeled with 3′ rhodamine. The complementary, antisense 5′ fluorescein-labeled ODN was quenched by the addition of the sense ODN. Formation of the hybrid from the injected ODNs was detected by FRET in the cytoplasm and in the cell nucleus. This suggested that antisense ODNs can hybridize to an intracellular target of exogenous origin, in both the cytoplasm and the nucleus.[76] In our study, the acceptor ODN is an oligonucleotide of defined sequence, which targets a previously determined sequence (the donor ODN). Each ODN is 20 nucleotides in length and has a GC content between 40% and 60%, which is ideal for FRET.[76] The donor ODN has been modified by the attachment of fluroescein at the 5′ end of the sequence (5′-/56-FAM/TCC CGC CTG TGA CAT GCA TT-3′), and the acceptor molecule has been modified by the attachment of rhodamine at the 3′ end of the strand (3′-/36-TAMNph/AG GGC GGA CAC TGT ACG TAA-5′). Fluorescence energy transfer occurs when the target sequence (donor), which is attached to the modified cell surface, forms a hybrid with the complementary sequence (acceptor). Figure 7A and B displays FRET between these two sequences at two molar ratios. The emission spectra demonstrate that after hybrid formation the fluorescence of fluorescein on the target strand is quenched and the energy is transferred to the acceptor molecule, which is on the 3′ end of the sequence,

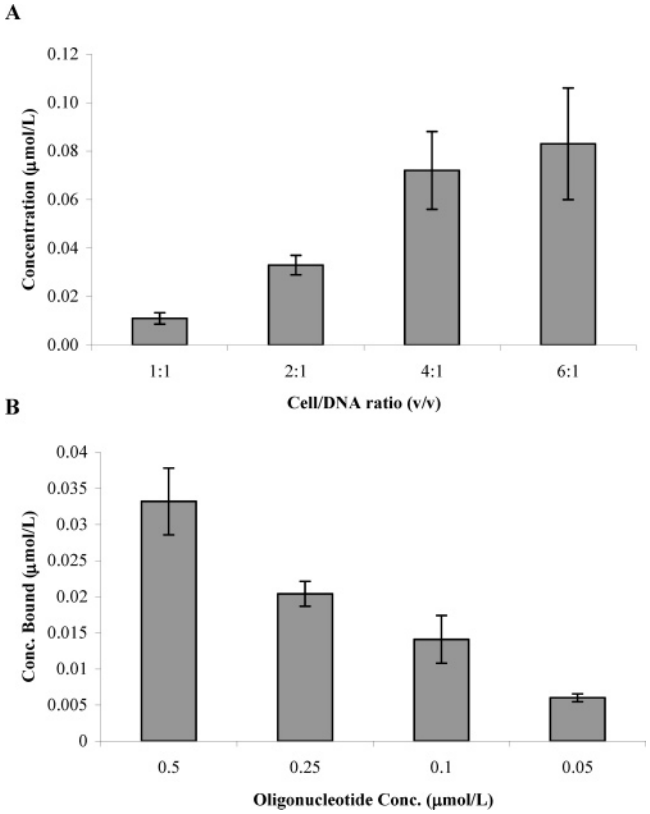

Figure 8. Hybrid formation between tethered ODN and its cy5-labeled complementary sequence. (A) Hybrid formation using modified cell to complementary ODN ratios of 1:1, 1:2, 1:4, and 1:6. Concentration of complementary ODN used is 5 μmol/L. (B) Hybridization at a range of oligonucleotide concentrations (0.05−0.5 μmol/L).

thus increasing the fluorescence of rhodamine. Calculations illustrated this and showed that at a molar ratio of 10:20 (donor:acceptor), Q = 92.3% and I = 52.5%, which suggests that fluorescein fluorescence was quenched by 92.3% and that the fluorescence of rhodamine was enhanced by 52.5% after hybrid formation, and at a molar ratio of 20:20, Q = 93.5% and I = 45.5%. At these two molar ratios, no concentration dependence is notable.

One concern with the FRET investigation is that any unattached donor ODN may react with acceptor ODN in solution, forming a hybrid. Therefore, these results may encompass binding at the cell surface plus binding in solution. To verify this point, in another type of hybridization assay we used the detection of cy5-labeled complementary ODN binding to its target sequence, which was attached to the outer shell of the cell−chitosan capsule. A series of modified cell to complementary ODN ratios were investigated (1:1, 1:2, 1:4, and 1:6 (v/v), Figure 8A). Data suggested that, as the number of encapsulated and ODN tethered cells increased, more and more of the cy5-labeled ODN is bound. This provides evidence for an increase in hybrid formation in the presence of an increasing number of binding sites. Figure 8B demonstrates that as the concentration of complementary ODN is increased there is a gradual increase in the formation of hybrids. Further work suggested that at a 1:1 ratio (cell:DNA) hybrid formation reached a plateau between 0.5 and 1 μmol/L.

IV. Conclusions

In this work, we reported on the ability of the LbL approach to physically and chemically alter cell surfaces and as an

immunocompatible coating, which could be used as biorecognition system. We have demonstrated the encapsulation of individual living cells, using different capsule formations based on natural polyelectrolytes, and we have shown that all systems form a stable complex around the cells. Cell viability and fluorescence studies confirmed that coated cells are still viable and in a healthy condition after polyelectrolyte deposition. This fact suggests that the capsules are biocompatible and noncytotoxic with respect to cell activity. TEM images indicated that cell morphology is not affected by the procedure or by the capsule. To extend the use of polyelectrolyte LbL encapsulation, research needs to focus on controlling cell division and maintaining the integrity of polyion layers.

LbL coating of DNA deposited onto polyelectrolyte (chitosan)-coated cells confirmed hybridization between tethered ODN and its complementary sequence. The stability of the system was ensured by four alternating layers of chitosan and DNA. Also, TEM images suggest the presence of polyelectrolyte clusters at the capsule surface and exponential growth of successive polyion layers.

The mechanism of layer growth is important when contemplating the use of such systems within the body because DNA or drug delivery systems require relatively stable complexes, with known amounts of DNA or drug contained within the system. Additional work is ongoing to analyze the mechanism of film growth, capsule architecture, and stability, and how these aspects affect the recognition properties of this system. We are also looking to accurately quantify the amount of DNA attached per capsule and the concentration of complimentary sequence required for hybrid formation. Preliminary investigations revealed the possibility of obtaining polyelectrolyte hollows with our systems by simply lyzing the cells. This would be an interesting avenue to follow, which would discard the need for harsh chemicals and extended preparation methods that are common when producing polyelectrolyte-based capsules. This approach might have applications in the field of protein, oligonucleotide, and gene delivery.

Acknowledgment. We would like to thank FQRNT-regroupement strategique through CBB for financial support. We also thank Dr. T. Veres from NRC-IMI laboratories for technical discussion of the potential application of the developed systems, and Dr. H. Vali, Dr. K. Sears, and Ms. J. Mui at the Facility for Electron Microscopy Research, McGill University, for guidance with TEM analysis.

References and Notes

(1) Decher, G. Fuzzy nanoassemblies: Toward layered polymeric multicomposites. *Science* **1997**, *277*, 1232−1237.
(2) Decher, G.; Schmitt, J. Fine-tuning of the film thickness of ultrathin multilayer films composed of consecutively alternating layers of anionic and cationic polyelectrolytes. *Prog. Colloid Polym. Sci*. **1992**, *89*, 160−164.
(3) Lvov, Y.; Decher, G.; Sukhoruko, G. Assembly of thin films by means of successive deposition of alternate layers of DNA and poly(allylamine). *Macromolecules* **1993**, *26*, 5396−5399.
(4) Lvov, Y.; Agria, K.; Ichinose, I.; Kunitake, T. Assembly of multicomponent protein films by means of electrostatic layer-by-layer adsorption. *J. Am. Chem. Soc*. **1995**, *117*, 6117−6123.
(5) Salditt, T.; Schubert, U. S. Layer-by-layer self-assembly of supramolecular and biomolecular films. *J. Biotechnol.* **2002**, *90*, 55−70.
(6) Zhu, H.; Ji, J.; Tan, Q.; Barbosa, M. A.; Shen, J. Surface engineering of poly(DL-lactide) via electrostatic self-assembly of extracellular matrix-like molecules. *Biomacromolecules* **2003**, *4*, 378−86.
(7) Ai, H.; Jones, S. A.; Lvov, Y. M. Biomedical applications of electrostatic layer-by-layer nano-assembly of polymers, enzymes, and nanoparticles. *Cell Biochem. Biophys.* **2003**, *39*, 23−43.
(8) Graul, T. W.; Schlenoff, J. B. Capillaries modified by polyelectrolyte multilayers for electrophoretic separations. *Anal. Chem.* **1999**, *71*, 4007−4013.
(9) Farhat, T. R.; Schlenoff, J. B. Ion transport and equilibria in polyelectrolyte multilayers. *Langmuir* **2001**, *17*, 1184−1192.
(10) Mamedov, A. A.; Kotov, N. A.; Prato, M.; Guldi, D. M.; Wicksted, J. P.; Hirsch, A. Molecular design of strong single-wall carbon nanotube/polyelectrolyte multilayer composites. *Nat. Mater.* **2002**, *1*, 190−194.
(11) Picart, C.; Gergely, C.; Arntz, Y.; Voegel, J. C.; Schaaf, P.; Cuisinier, F. J.; Senger, B. Measurement of film thickness up to several hundreds of nanometers using optical waveguide lightmode spectroscopy. *Biosens. Bioelectron.* **2004**, *20*, 553−561.
(12) Zhang, J.; Senger, B.; Vautier, D.; Picart, C.; Schaaf, P.; Voegel, J. C.; Lavalle, P. Natural polyelectrolyte films based on layer-by layer deposition of collagen and hyaluronic acid. *Biomaterials* **2005**, *26*, 3353−3361.
(13) Fu, J.; Ji, J.; Yuan, W.; Shen, J. Construction of anti-adhesive and antibacterial multilayer films via layer-by-layer assembly of heparin and chitosan. *Biomaterials* **2005**, *26*, 6684−6692.
(14) Gong H, H.; Garcia-Turiel, J.; Vasilev, K.; Vinogradova, O. I. Interaction and adhesion properties of polyelectrolyte multilayers. *Langmuir* **2005**, *21*, 7545−7550.
(15) Decher, G.; Hong, J. D.; Schmitt, J. Buildup of ultrathin multilayer films by a self-assembly process: III. Consecutively alternating adsorption of anionic and cationic polyelectrolytes on charged surfaces. *Thin Solid Films* **1992**, *210/211*, 831−835.
(16) Li, B.; Haynie, D. T. Multilayer biomimetics: reversible covalent stabilization of a nanostructured biofilm. *Biomacromolecules* **2004**, *5*, 1667−1670.
(17) Kim, D. K.; Han, S. W.; Kim, C. H.; Hong, J. D.; Kim, K. Morphology of multilayers assembled by electrostatic attraction of oppositely charged model polyelectrolytes. *Thin Solid Films* **1999**, *350*, 153−160.
(18) Sukhishvili, S. A. Layered, erasable polymer multilayers formed by hydrogen-bonded sequential self-assembly. *Macromolecules* **2002**, *35*, 301−310.
(19) McAloney, R. A.; Sinyor, M.; Dudnik, V.; Goh, M. C. Atomic force microscopy studies of salt effects on polyelectrolyte multilayer film morphology. *Langmuir* **2001**, *17*, 6655−6663.
(20) McAloney, R. A.; Dudnik, V.; Goh, M. C. Kinetics of salt-induced annealing of a polyelectrolyte multilayer film morphology. *Langmuir* **2003**, *19*, 3942−3952.
(21) Lavalle, Ph.; Gergely, C.; Cuisinier, F. J. G.; Dercher, G.; Schaaf, P.; Voegel, J. C.; Picart, C. Comparison of the structure of polyelectrolyte multilayer films exhibiting a linear and an exponential growth regime: An in situ atomic force microscopy study. *Macromolecules* **2002**, *35*, 4458−4465.
(22) Decher, G.; Hong, J. D. Buildup of ultrathin multilayer films by a self-assembly process: I. Consecutive adsorption of anionic and cationic bipolar amphiphiles and polyelectrolytes on charged surfaces. *Ber. Bunsen-Ges. Phys. Chem.* **1991**, *95*, 1430−1439.
(23) Sukhorukov, G. B.; Mohwald, H.; Decher, G.; Lvo, Y. M. Assembly of polyelectrolyte multilayer films by consecutively alternating adsorption of polynucleotides and polycations. *Thin Solid Films* **1996**, *284−285*, 220−223.
(24) Park, M. K.; Deng, S.; Advincula, R. C. pH-Sensitive bipolar ion-permselective ultrathin films. *J. Am. Chem. Soc.* **2004**, *126*, 13723−31.
(25) Decher, G.; Lehr, B.; Lowack, K.; Lvov, Y.; Schmidt, J. New nanocomposite films for biosensors: layer-by-layer adsorbed films of polyelectrolytes, proteins or DNA. *Biosens. Bioelectron.* **1994**, *9*, 677−684.
(26) He, P. G.; Takahashi, T.; Hoshi, T.; Anzai, J.-I.; Suzuki, Y.; Osa, T. Preparation of enzyme multilayers on electrode surface by use of avidin and biotin-labled enzyme for biosensor applications. *Mater. Sci. Eng., C* **1994**, *2*, 103−106.
(27) Caruso, F.; Caruso, R. A.; Mohwald, H. Nanoengineering of inorganic and hybrid hollow spheres by colloidal templating. *Science* **1998**, *282*, 1111−1114.
(28) Shenoy, D. B.; Antipov, A. A.; Sukhorukov, G. B.; Mohwald, H. Layer-by-layer engineering of biocompatible, decomposable core−shell structures. *Biomacromolecules* **2003**, *4*, 265−72.
(29) Pargaonkar, N.; Lvov, Y. M.; Li, N.; Steenekamp, J. H.; de Villiers, M. M. Controlled release of dexamethasone from microcapsules produced by polyelectrolyte layer-by-layer nanoassembly. *Pharm Res.* **2005**, *22*, 826−835.

(30) Yap, H. P.; Quinn, J. F.; Ng, S. M.; Cho, J.; Caruso, F. Colloid surface engineering via deposition of multilayered thin films from polyelectrolyte blend solutions. *Langmuir* **2005**, *21*, 4328−33.
(31) Zhang, Y.; Guan, Y.; Zhou, S. Single component chitosan hydrogel microcapsule from a layer-by-layer approach. *Biomacromolecules* **2005**, *6*, 2365−2369.
(32) Peyratout, C. S.; Dahne, L. Tailor-made polyelectrolyte microcapsules: from multilayers to smart containers. *Angew. Chem., Int. Ed.* **2004**, *43*, 3762−3783.
(33) Radtchenko, I. L.; Sukhorukov, G. B.; Leporatti, S.; Khomutov, G. B.; Donath, E.; Mohwald, H. Assembly of alternated multivalent ion/polyelectrolyte layers on colloidal particles. Stability of the multilayers and encapsulation of macromolecules into polyelectrolyte capsules. *J. Colloid Interface Sci.* **2000**, *230*, 272−280.
(34) Sukhorukov, G. B.; Antipov, A. A.; Voigt, A.; Donath, E.; Mohwald, H. pH-controlled macromolecule encapsulation in and release from polyelectrolyte multilayer nanocapsules. *Marcomol. Rapid Commun.* **2001**, *22*, 44−46.
(35) Neu, B.; Voigt, A.; Mitlohner, R.; Leporatti, S.; Gao, C. Y.; Donath, E.; Kiesewetter, H.; Mohwald, H.; Meiselman, H. J.; Baumler, H. Biological cells as templates for hollow microcapsules. *J. Microencapsulation* **2001**, *18*, 385−395.
(36) Caruso, F.; Trau, D.; Mohwald, H.; Renneberg, R. Enzyme encapsulation in layer-by-layer engineered multilayer capsules. *Langmuir* **2000**, *16*, 1485−1488.
(37) Lvov, Y.; Caruso, F. Biocolloids with ordered urease multilayer shells as enzymatic reactors. *Anal. Chem.* **2001**, *73*, 4212−4217.
(38) Khopade, A. J.; Caruso, F. Stepwise self-assembled poly(amidoamine) dendrimer and poly(styrenesulfonate) microcapsules as sustained delivery vehicles. *Biomacromolecules* **2002**, *3*, 1154−1162.
(39) Glinel, K.; Prevot, M.; Krustev, R.; Sukhorukov, G. B.; Jonas, A. M.; Mohwald, H. Control of the water permeability of polyelectrolyte multilayers by deposition of charged paraffin particles. *Langmuir* **2004**, *20*, 4898−4902.
(40) Volodkin, D. V.; Petrov, A. I.; Prevot, M.; Sukhorukov, G. B. Matrix polyelectrolyte microcapsules: new system for macromolecule encapsulation. *Langmuir* **2004**, *20*, 3398−3406.
(41) Gittins, D. I.; Caruso, F. Multilayered polymer nanocapsules derived from gold nanoparticle templates. *Adv. Mater.* **2000**, *12*, 1947−1949.
(42) Caruso, F. Nanoengineering of particle surfaces. *Adv. Mater.* **2001**, *13*, 11−21.
(43) Sukhorukov, G. B.; Donath, E.; Moya, S.; Susha, A. S.; Voigt, A.; Hartmann, J.; Mohwald, H. Microencapsulation by means of stepwise adsorption of polyelectrolytes. *J. Microencapsulation* **2000**, *17*, 177−185.
(44) Hua, A.; Fang, M.; Jones, S. A.; Lvov, Y. M. Electrostatic layer-by-layer nanoassembly on biological microtemplates: platelets. *Biomacromolecules* **2002**, *3*, 560−564.
(45) Bhadra, D.; Gupta, G.; Bhadra, S.; Umamaheshwain, R. B.; Jain, N. K. Multicomposite ultrathin capsules for sustained ocular delivery of ciprofloxacin hydrochloride. *J. Pharm. Pharm. Sci.* **2004**, *7*, 241−251.
(46) Krol, S.; Diaspro, A.; Magrassi, R.; Ballario, P.; Grimaldi, B.; Filetici, P.; Ornaghi, P.; Ramoino, P.; Gliozzi, A. Nanocapsules: coating for living cells. *IEEE Trans. Nanobiosci.* **2004**, *3*, 32−38.
(47) Diaspro, A.; Silvano, D.; Krol, S.; Cavalleri, O.; Gliozzi, A. Single living cell encapsulation in nano-organized polyelectrolyte shells. *Langmuir* **2002**, *18*, 5047−5050.
(48) Mak, W. C.; Sum, K. W.; Trau, D.; Renneberg, R. Nanoscale surface engineered living cells with extended substrate spectrum. *IEEE Proc. Nanotechnol.* **2004**, *151*, 67−72.
(49) Richert, L.; Lavalle, P.; Payan, E.; Shu, X. Z.; Prestwich, G. D.; Stoltz, J. F.; Schaaf, P.; Voegel, J. C.; Picart, C. Layer by layer buildup of polysaccharide films: physical chemistry and cellular adhesion aspects. *Langmuir* **2004**, *20*, 448−458.
(50) Hammond, P. T.; Whitesides, G. M. Formation of polymer microstructures by selective deposition of polyion multilayers using patterned self-assembled monolayers as a template. *Macromolecules* **1995**, *28*, 7569−7571.
(51) Keller, S. W.; Johnson, S. A.; Brigham, E. S.; Yonemoto, E. H.; Mallouk, T. E. Photoinduced charge separation in multilayer thin films grown by sequential adsorption of polyelectrolytes. *J. Am. Chem. Soc.* **1995**, *117*, 12879−12880.
(52) Huang, M.; Ma, Z. S.; Khar, E.; Lim, L.-Y. Uptake of FITC-chitosan nanoparticles by A549 cells. *Pharm. Res.* **2002**, *19*, 1488−1494.
(53) Thierry, B.; Winnik, F. M.; Merhi, Y.; Silver, J.; Tabrizian, M. Bioactive coatings of endovascular stents based on polyelectrolyte multilayers. *Biomacromolecules* **2003**, *4*, 1564−1571.
(54) Thierry, B.; Winnik, F. M.; Merhi, Y.; Tabrizian, M. Nanocoatings onto arteries via layer-by-layer deposition: Toward the in vivo repair of damaged blood vessels. *J. Am. Chem. Soc.* **2003**, *125*, 7494−7495.
(55) dos Santos, D. S., Jr.; Bassi, A.; Rodrigues, J. J., Jr.; Misoguti, L.; Oliveira, O. N., Jr.; Mendonca, C. R. Light-induced storage in layer-by-layer films of chitosan and an azo dye. *Biomacromolecules* **2003**, *4*, 1502−1505.
(56) Quarrant-ul-Ain; Sharma, S.; Khuller, G. K.; Garg, S. K. Alginate-based oral drug delivery system for tuberculosis: pharmacokinetics and therapeutic effects. *J. Antomicrob. Chemother.* **2003**, *51*, 931−938.
(57) Gu, F.; Amsden, B.; Neufeld, R. Sustained delivery of vascular endothelial growth factor with alginate beads. *J. Controlled Release* **2004**, *96*, 463−472.
(58) Dai, C.; Wang, B.; Zhao, H.; Li, B. Factors affecting protein release from microcapsule prepared by liposome in alginate. *Colloids Surf., B* **2005**, *42*, 253−258.
(59) Balakrishman, B.; Jayakrishman, A. Self-cross-linking biopolymers as injectable in situ forming biodegradable scaffolds. *Biomaterials* **2005**, *26*, 3941−3951.
(60) Thierry, B.; Winnik, F.; Merhi, Y.; Silver, J.; Tabrizian, M. Radionuclides-hyaluronan-conjugate thromboresistant coatings to prevent in-stent restenosis. *Biomaterials* **2004**, *25*, 3895−3905.
(61) Thierry, B.; Faghihi, S.; Torab, L.; Pike, B.; Tabrizian, M. Magnetic resonance signal-enhancing self-assembled coating for endovascular devices. *Adv. Mater.* **2005**, *17*, 826−830.
(62) Cuero, R. G. Enhanced heavy metal immobilization by a bacterial-chitosan complex in soil. *Biotechnol. Lett.* **1996**, *18*, 511−514.
(63) Finlay, B. B.; Cossart, P. Exploitation of mammalian host cell functions by bacterial pathogens. *Science* **1997**, *276*, 718−725.
(64) Gruenberg, J.; Gisou van der Goot, F. Mechanisms of pathogen entry through the endosomal compartments. *Nat. Rev.: Mol. Cell Biol.* **2006**, *7*, 495−504.
(65) Erokhin, V.; Popov, B.; Samori, B.; Yakovlev, A. Immobilization of DNA fragments by Langmuir−Blodgett technique. *Mol. Cryst. Liq. Cryst.* **1992**, *215*, 213−220.
(66) Lindman, B.; Mel'nikov, S.; Mel'nikov, Y.; Nylander, T.; Eskilsson, K.; Miguel, M.; Dias, R.; Leal, C. DNA-lipid systems. An amphiphile self-assembly and polymer-surfactant perspective. *Prog. Colloid Polym. Sci.* **2002**, *120*, 52−63.
(67) Caruso, F. Hollow capsule processing through colloidal templating and self-assembly. *Chem.-Eur. J.* **2000**, *6*, 413−419.
(68) Schuler, C.; Caruso, F. Decomposable hollow biopolymer-based capsules. *Biomacromolecules* **2001**, *2*, 921−926.
(69) Caruso, F.; Yang, W.; Trau, D.; Renneberg, R. Microcapsulation of uncharged low molecular weight organic materials by polyelectrolyte multilayer self-assembly. *Langmuir* **2000**, *16*, 8932−8936.
(70) Caruso, F.; Schuler, C.; Kurth, D. G. Core−shell particles and hollow shells containing metallo-supramolecular components. *Chem. Mater.* **1999**, *11*, 3394−3399.
(71) Sukhorukov, G. B.; Donath, E.; Lichtenfed, H.; Knippel, E.; Knippel, M.; Budde, A.; Mohwald, H. Layer-by-layer self-assembly of polyelectrolytes on colloidal particles. *Colloids Surf., A* **1998**, *137*, 253−266.
(72) Feng, Q.; Zeng, G.; Yang, P.; Wang, C.; Cai, J. Self-assembly and characterization of polyelectrolyte complex films of hyaluronic acid/chitosan. *Colloids Surf., A* **2005**, *257−258*, 85−88.
(73) Decher, G. In *Comprehensive Supramolecular Chemistry: Templating, Self-Assembly and Self-Organization*; Sauvage, J. P., Hosseini, M. W., Eds.; Pergamon Press: Oxford, 1996; Vol. 9, pp 507−528.
(74) Diaspro, A.; Krol, S.; Cavalleri, O.; Gliozzi, A. Nano-organized polyelectrolyte shells. Coating for living cells and tissues. Tissue engineering. *BIOforum Eur.* **2005**, *6*, 2−3.
(75) Bjornson, K. P.; Amaratunga, M.; Moore, K. J. M.; Lohman, T. M. Single-turnover kinetics of helicase-catalyzed DNA unwinding monitored continuously by fluorescence energy transfer. *Biochemistry* **1994**, *33*, 14306−14316.
(76) Sixou, S.; Szoua, F. C., Jr.; Green, G. A.; Giusti, B.; Zon, G.; Chin, D. J. Intracellular oligonucleotide hybridisation detected by fluorescence resonance energy transfer (FRET). *Nucleic Acids Res.* **1994**, *22*, 662−668.
(77) Cardullo, R. A.; Agrawal, S.; Flores, C.; Zamecnik, P. C.; Wolf, D. E. Detection of nucleic acid hybridisation by nonradiative fluorescence resonance energy transfer. *Proc. Natl. Acad. Sci. U.S.A.* **1998**, *85*, 8790−8794.

BM060266J